Mild Hypobaric Hypoxia Effects on Murine Skeletal Muscle Morphology and Macrophages and Well-Being

Liyuan Zhang; Julia Soulakova; Barbara St. Pierre Schneider

BACKGROUND: In the last 10 yr, the number of ultra-haul flights—defined as flights greater than 12 h of flying time—has increased. While the medical complications of these flights are well-known, the underlying cellular effects are less clear. The primary objective of this study was to test the effects of extended mild hypobaric hypoxia on overall well-being and skeletal muscle morphology and macrophage populations.

METHODS: A total of 22 male C57BL/6 mice were assigned to a normobaric (NB) or hypobaric (HB) chamber for 14–17 h. Overall mouse well-being and the general morphology and resident macrophage number in hindlimb muscles were compared between the two pressure conditions.

RESULTS: During mild hypobaric hypoxia, the mice behaved normally and no changes were observed in general muscle morphology. Regarding resident macrophages, the mean antigen area of CD206 in the hindlimb muscles, lateral gastrocnemius (LG, 33.8 $\pm$ 2.0 vs. 35.3 $\pm$ 1.6), medial gastrocnemius (MG, 32.4 $\pm$ 1.6 vs. 32.6 $\pm$ 1.5), and quadriceps femoris (QF, 36.3 $\pm$ 1.2 vs. 34.3 $\pm$ 1.1) were similar between NB and HB conditions, and the number of CD68-positive cells in the LG and QF were similar between the two conditions. Significantly fewer CD206-positive cells were counted in the LG muscle under the HB condition.

CONCLUSION: Our findings indicate that extended exposure to mild hypobaric hypoxia, similar to that of an ultra-long-haul flight, does not adversely affect healthy skeletal muscle.

KEYWORDS: CD206, quadriceps femoris.

Zhang L, Soulakova J, St. Pierre Schneider B. *Mild hypobaric hypoxia effects on murine skeletal muscle morphology and macrophages and well-being*. Aerosp Med Hum Perform. 2019; 90(12):1050–1054.

With the presence of more fuel-efficient aircraft, reduced oil prices, and increased demand from business passengers, ultra-long-haul airline flights—defined as flights greater than 12 h of flying time—are experiencing a resurgence.[8] According to Engel,[5] only 10 flights exceeding 8000 miles (~12,875 km or 16 h of flight time) were scheduled in 2008, whereas 26 of these flights were offered in October 2018. Current examples of this type of travel include flights from Doha to Auckland (~17 h and 14,536 km) or Singapore to New York (~18 h and 15,345 km).[8,12] However, the longest flight in this category, nonstop service from Sydney or Melbourne to London and New York,[4] will be available to consumers in the near future. As airlines are cultivating plans to increase the availability of ultra-long-haul flights, discussions concerning passenger comfort and health, including its effects on various medical conditions (e.g., airsickness, anemia, diabetes), are becoming more prevalent in public literature.[1,14]

Although the medical complications of long haul (6–12 h duration) and ultra-long-haul (>12 h duration) flights are well-known,[11] only one ultra-long-haul study examining acute physiological effects has been conducted to our knowledge. Muhm et al. simulated a 20-h flight at different altitudes and examined discomfort and arterial oxygen saturation in adult volunteers.[6] At 8000 ft (2438 m) above sea level, which represents a mild hypobaric hypoxic state, a reduction of 4.4 percentage points in mean arterial oxygen saturation was reported along with increased ratings of muscular discomfort.[6]

In contrast, more data regarding acute cellular or genetic effects of long-haul flights are available. Wilder-Smith et al.

From the School of Nursing, University of Nevada, Las Vegas, NV, and the Burnett School of Biomedical Sciences, University of Central Florida, Orlando, FL.

This manuscript was received for review in January 2019. It was accepted for publication in September 2019.

Address correspondence to: Barbara St. Pierre Schneider, University of Nevada, Las Vegas, Las Vegas, NV 89154-3018; barbara.stpierreschneider@unlv.edu.

DOI: https://doi.org/10.3357/AMHP.5333.2019

investigated the effects of a 10-h simulated flight on two stress biomarkers, nine white blood cell antigens, and one immune function test in men and women.[15] Immediately after the flight, the major findings were a reduction in immune function, indicated by the lymphocyte mitogen proliferation assay and increased white blood cell expression of the CD14 antigen.[15] St. Pierre Schneider et al. reported on genetic expression and inflammatory indicators in skeletal muscle after ~8–9 h of simulated flight.[9] In the muscle of male mice, four noncoding RNA genes were upregulated, whereas in female mice, 14 protein coding genes were downregulated, including genes related to epithelial homeostasis and those related to cellular damage.[9] However, simulated flight had no effect on inflammatory indicators in the muscle, including proinflammatory cytokine genes and white blood cells markers.[9] Further, Reis et al. found a higher prevalence of self-reported sleep disturbances and lower fatigue occurrence in pilots who flew long-haul flights compared to those who flew short/medium-haul flights.[7] These findings suggest differential changes could occur during or after ultra-long-haul flights. With the current operation of these flights and the ongoing interest in aircraft occupant safety and comfort, additional biomedical research regarding ultra-long-haul flights is needed.[2]

As part of this inquiry, skeletal muscle is an appropriate target to study. Since 45% of the body is comprised of this tissue, muscular discomfort could occur during ultra-long-haul flight.[6] Skeletal muscle also contains resident immune cells, or macrophages, which express antigens sensitive to hypoxia.[13] Therefore, the primary objective of this study was to test the effect of extended mild hypobaric hypoxia on overall physiological functioning, skeletal muscle morphology, and muscle resident macrophage populations in mice.

METHODS

Animals

All animal procedures were approved by the University of Nevada, Las Vegas, Institutional Animal Care and Use Committee and the U.S. Army Medical Research and Materiel Command Animal Care and Use Review Office. Animals were maintained under the surveillance of a veterinarian and other personnel in a specific pathogen-free Association for Assessment and Accreditation of Laboratory Animal Care International-accredited facility at the University of Nevada, Las Vegas. This facility requires that all mouse research abide by the *Guide for the Care and Use of Laboratory Animals* and the Office of Laboratory Animal Welfare. Male ($N = 22$) C57BL/6 mice (approximately 6 wk old and 20 g) were purchased from Envigo Laboratories (Indianapolis, IN) and allowed at least 5 d to acclimate before the start of the study. The facility used an individually ventilated caging system and mice were group housed [4–5 mice per ventilated cage (Lab Products, Seaford, DE)] under a 12:12-h light:dark cycle. Animals were fed a standard laboratory diet with food and water ad libitum.

Procedure

Mice were evenly assigned to exposure to normobaria or hypobaria for 14–17 h. Normobaric (NB) conditions were defined as ambient laboratory atmospheric pressure in Las Vegas [700−726 mmHg, 2001.3 ft (610 m) elevation], and hypobaric (HB) conditions were targeted to 565 ± 5 mmHg, equivalent to an altitude of 8000 ft (2438 m). Each exposure occurred in an acrylic chamber as described previously[9] and the mice did not undergo any prescribed exercise regimen during the exposure. Bodyweight was measured before placement in the chamber and the chamber was de-pressurized over a 10–15-min time span to reach the target pressure. Each mouse was visually monitored 30 min after chamber placement and each hour thereafter for quality and depth of respirations, mouth color, posture, and activity level. If the quality or depth of respirations of a mouse during the chamber time was questioned, another mouse undergoing NB exposure at the same time was used as a comparison. Unacceptable conditions related to respiration were pale or bluish mouth color (as opposed to pink or red) and a hunched back posture. Chamber pressure was monitored and the CO_2 level (ppm) was measured to verify that CO_2 was not accumulating in the chamber,[9] then the CO_2 level was converted to partial pressure. At the end of the exposure period, each mouse was removed from the chamber, weighed, and then euthanized.

Each mouse was anesthetized with inhalant isoflurane (1–5%) and 100% oxygen and euthanized by cervical dislocation. Following euthanasia, the plantarflexor (medial and lateral gastrocnemius, plantaris, and soleus) and quadriceps femoris (QF) muscles were harvested. The muscles were frozen in melting isopentane (Fisher Scientific, Pittsburgh, PA), cooled by liquid nitrogen. All frozen muscles for macrophage analysis were then stored at −70°C. In addition, the spleen was harvested and weighed post-euthanasia to determine whether splenomegaly occurred after HB exposure.

Serial cross-sections 10 microns thick at or near the midbelly of the gastrocnemius and QF muscles were cut using a cryostat (Leica CM1850, Leica Microsystems Inc., Bannockburn, IL). Cross-sections were applied to positively charged or poly-L-lysine-coated slides and stored at −70°C until immunolabeling. In addition, cross-sections were fixed in methanol and stained with hematoxylin and eosin for morphological analysis.

Following a similar procedure previously described,[10] immunolabeling was used to detect the presence of macrophages in frozen muscle cross-sections. The primary monoclonal antibodies were rat antimouse CD206 (MR5D3, 1:100; Bio-Rad, Hercules, CA), rat antimouse CD68 (FA-11, 1:100; Bio-Rad), rabbit antimouse CD163 (EPR19518, 1:20; Abcam, Cambridge, MA), and rat antimouse F4/80 (BM8, 1:20; Invitrogen, Frederick, MD). Control sections were generated as described above, except the primary antibody step was substituted by immersing the sections in phosphate-buffered saline for 2 h.

To quantify the anti-CD206 and anti-CD68 antibody immunolabeling, one image of a region of interest (ROI; identified as an area with the most cells) was captured using a 10× objective

(100× magnification) attached to an Eclipse E600 light microscope (Nikon Inc., Melville, NY), a Retiga 2000R CCD Camera (QImaging, Surrey, BC, Canada), and Image-Pro® Premier 9.2 software (Media Cybernetics Inc., Silver Spring, MD). Point background correction was performed with Image-Pro® Premier 9.2 software. Each image represented one ROI. A total of 42 lateral gastrocnemius (LG), 21 medial gastrocnemius (MG), and 22 QF images were captured. In addition, an image from control sections was matched with the corresponding immunolabeled section. Any unmatched area was removed from the analysis, and the range of the adjusted ROIs was 0.70–1.02 $mm.^2$ Each positive object was considered a positive cell. The following positive objects were excluded after confirmation by a second observer and thresholding: debris; positive objects partially located within an ROI; and positive objects located in the epimysium surrounding the LG, MG, or QF or on the edge of the section. To determine the threshold, three cells with medium intense staining and one cell with weak staining were identified. A threshold number was then selected to ensure the three cells with medium intense staining were counted and the cell with weak staining was excluded. A second observer conducted a ground truth analysis using 5 randomly selected images from each muscle (a total of 15 images). The false-positive rate was 5%. The variables quantified for the LG, MG, or QF muscles were the number of positive cells (total number of positive objects per mm^2 per ROI) and the mean antigen area of positive cells per ROI.

To detect the distribution of the CD206-positive cells within the perimysium or endomysium of QF cross-sections, fluorescent immunolabeling was performed. The primary and corresponding secondary antibodies were rat antimouse CD206 and Alexa Fluor 488 goat antirat IgG (1:250; ThermoFisher Scientific, Rockford, IL) and rabbit antimouse collagen III (1:100; ThermoFisher Scientific) and Alexa Fluor 546 goat antirabbit IgG (1:250; ThermoFisher Scientific). Slides were mounted with ProLong™ Diamond Antifade Mountant with DAPI (ThermoFisher Scientific) and visualized. The perimysium was identified by the thicker, brighter collagen III labeling outlining bundles of three or more muscle fibers. The endomysium was identified by the thinner, dimmer collagen III labeling surrounding individual muscle fibers.

Statistical Analyses

For all statistical analyses, the confidence level and alpha were set at 95% and 5%, respectively. Outcomes were treated independently. When comparing the means, the normality assumption was checked using the Q-Q plots, and then the Folded test for equality of variances was performed. If the assumption of equal variances was supported, then the pooled variance estimation approach was used. Otherwise, the Satterthwaite method was used. A 95% confidence interval based on the *t*-distribution was constructed for mean differences. If the confidence interval contained zero, then we concluded no significant difference between the means. The medians of the 1) absolute differences of bodyweight before (BW1) and after (BW2) exposure to normobaria or mild hypobaric hypoxia and 2) rates of change in bodyweight (|BW1-BW2|/BW1) were analyzed by Wilcoxon signed-rank test. A repeated measures analysis of variance with Greenhouse-Geisser correction was performed to determine the relationship of chamber pressure and time with chamber CO_2 levels and time. Values are mean ± SE.

RESULTS

During the experiment, the NB chamber pressure ranged from 700–727 mmHg, and the HB chamber pressure ranged from 563–570 mmHg. During the 14–17-h chamber exposure, the mean pressure remained stable in both the NB and HB chambers ($P = 0.31$); however, the mean pressure was lower in the HB chamber than in the NB chamber ($P < 0.001$). Across the exposure period, the changes in the mean CO_2 partial pressure were different for both the NB and HB conditions ($P < 0.001$), with the NB chamber ranging from 0.29–0.38 Pa and 0.19–0.23 Pa in the HB chamber.

During and after HB and NB exposure, the mice exhibited normal respirations, mouth color, and posture. Piloerection of fur was not observed. While the mice were inside the HB and NB chambers, they behaved normally (i.e., nesting, sleeping, grooming, eating, and drinking water).

Although the bodyweight change was only approximately 4% on average for each group and statistically significant for each group ($P < 0.0001$), the rate of bodyweight change was similar for both exposure conditions. Furthermore, the absolute differences of the bodyweight before and after pressure exposure did not differ significantly between the two conditions.

Mean relative spleen weight was similar between NB (mean = $2.56\ mg \cdot g^{-1}$, SE = $0.24\ mg \cdot g^{-1}$) and HB (mean = $2.42\ mg \cdot g^{-1}$, SE = $0.24\ mg \cdot g^{-1}$) conditions. The 95% confidence interval for the mean relative spleen weight difference between the two conditions is –0.07, 0.35.

For both conditions, muscle fibers exhibited no variation in eosin staining. In addition, nuclei were primarily located peripherally around muscle fibers. Therefore, no evidence of inflammation was observed in the muscles exposed to mild hypobaric hypoxia (**Fig. 1**).

CD206-positive cells varied in shape and size and exhibited an overall strong intensity (**Fig. 2A and B**). CD206-positive cells in QF cross-sections were observed within the perimysium (90% ± 2.4%) and endomysium ($N = 4$ mice, 10% ± 2.4%, **Suppl. Fig. A1 A–C**, online at https://doi.org/10.3357/AMHP.5333sd.2019). The mean number of CD206-positive cells in LG muscle was 22% lower under the HB condition than in the NB condition, but no significant difference in the number was detected in the QF and MG muscles (**Fig. 3A**). No difference in mean CD206 antigen area (**Fig. 3B**) was observed between the NB and HB conditions for the QF, LG, and MG muscles.

The CD68-positive cells were located near the periphery of muscle fibers and had an elongated or roundish shape. For the LG and QF muscles, no difference in the mean number of

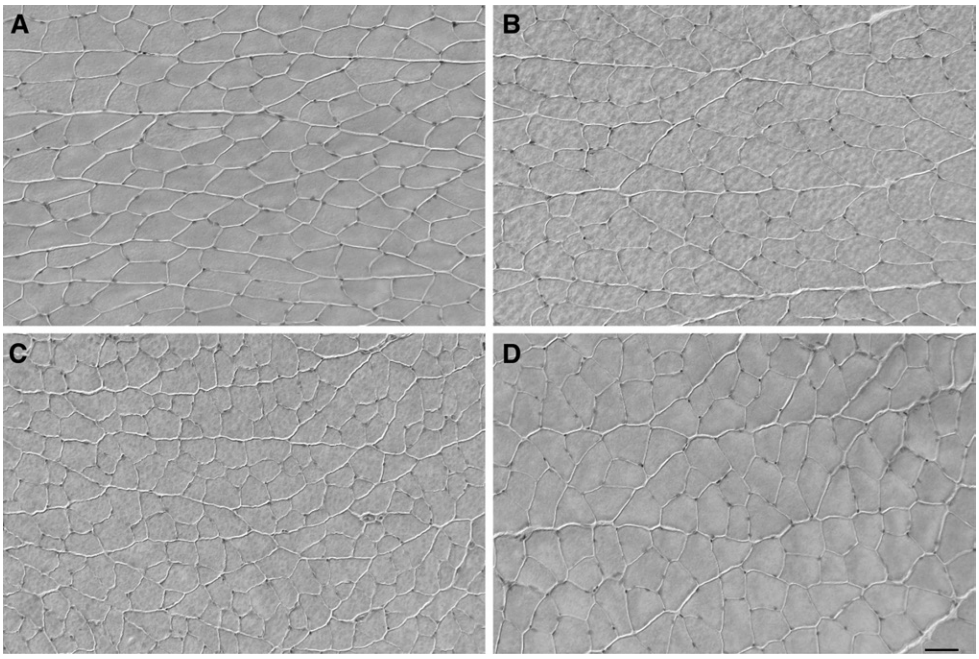

Fig. 1. Morphology of mouse LG (A, C) and QF (B, D) muscle cross-sections after exposure to NB (A, B) and HB (C, D) conditions. Hematoxylin and eosin, bar = 50 µm. LG = lateral gastrocnemius; QF = quadriceps femoris; NB = normobaric; HB = mild hypobaric.

CD68-positive cells (**Fig. 3C**) and mean antigen area was observed between the NB and HB conditions.

The F4/80 protein was absent around muscle fibers in seven LG muscle cross-sections (NB, $N = 5$; HB, $N = 2$). In three QF muscle cross-sections (NB, $N = 3$), the CD163 protein was absent around muscle fibers, but present in thick connective tissue near the vastus lateralis, which is one of the four QF muscles.

DISCUSSION

This study evaluated the effect of mild hypobaric hypoxia for a period of time similar to that of an ultra-long-haul flight on murine muscle, spleen, and overall well-being. During 14–17 h of exposure to an atmospheric pressure equivalent to an altitude of 8000 ft (2438 m), these mice demonstrated normal behavior, respiratory rate, and posture. Regarding immune parameters, spleen weight was normal, and the only difference in muscle resident macrophages between the two pressure conditions was in the number of CD206-positive cells. These cells were observed to be fewer in number in the LG muscle under the HB condition than in the NB condition; however, since the general muscle morphology of this muscle appeared normal, we infer that fewer CD206-positive macrophages did not affect the overall health of the muscle fibers. Therefore, these findings suggest that an ultra-long-haul flight does not adversely affect the overall integrity and inflammatory status of healthy skeletal muscle.

Building upon these results and the findings of others,[7,9,15] additional areas to investigate relate to pilot labor variables and passenger health. For example, this or another simulated flight model could be used to compare the effects of flying duration, early starts, or night periods on overall immune function and skeletal muscle health, including the population of resident macrophages and muscle metabolism. This research will enhance our understanding of the interaction of pilot labor variables, exposure to mild hypobaric hypoxia, and physiological functioning with the long-term objective of optimizing pilot health and well-being. Furthermore, as potential and current passengers of ultra-long-haul flights have offered health and wellness suggestions (e.g., space to perform exercise), simulated flight studies may aid in designing optimal exercise regimens at an altitude of 8000 ft (2438 m).[3]

With multiple perspectives from airlines, pilots, flight crew, and passengers related to general experiences and concerns associated with ultra-long-haul flights, advances in understanding mild hypobaric hypoxic effects are needed more than ever. These advances can be achieved both through mouse and human studies, resulting in an enriched aerospace medicine knowledge base.

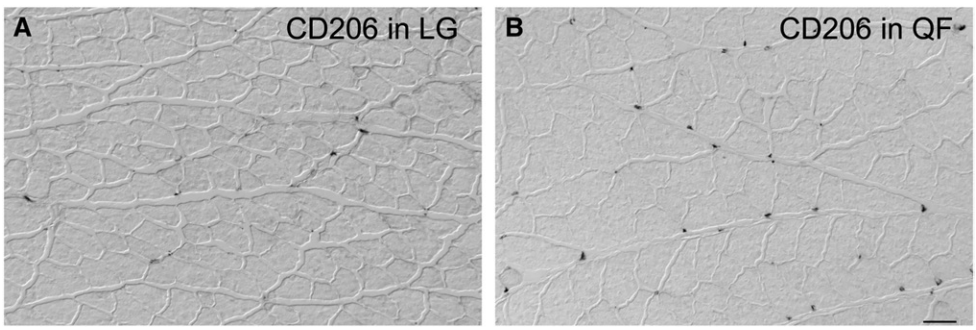

Fig. 2. CD206-positive cells in A) LG and B) QF cross-sections after HB exposure. LG = lateral gastrocnemius; QF = quadriceps femoris; HB = mild hypobaria, 50 µm.

ACKNOWLEDGMENTS

The authors would like to thank Sarah Lyons for editorial assistance.

Financial Disclosure Statement: The authors have no competing interests to declare.

The U.S. Army Medical Research Acquisition Activity, Fort Detrick, MD,

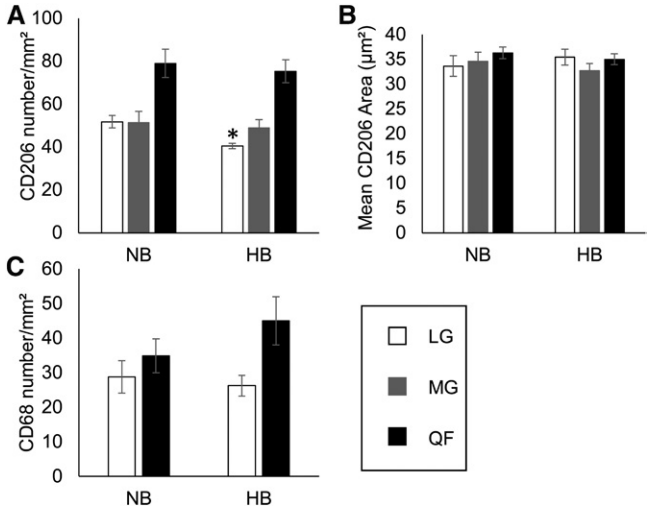

Fig. 3. Quantification of CD206 and CD68 in mouse LG, MG, and QF muscle cross-sections after exposure to NB and HB conditions. A) CD206 number/mm^2 and B) mean CD206 antigen area. *LG muscle, NB vs. HB conditions ($P < 0.05$). C) CD68 number/mm^2. NB = normobaric; HB = mild hypobaric; LG = lateral gastrocnemius; MG = medial gastrocnemius; QF = quadriceps femoris. For statistical analyses, group sizes = 10–11. Values are mean ± SE.

is the awarding and administering acquisition office of this research. This work was supported by the Assistant Secretary of Defense for Health Affairs through the Joint Warfighter Medical Research Program under Award No. W81XWH-16-1-0150. Opinions, interpretations, conclusions, and recommendations are those of the author and are not necessarily endorsed by the Department of Defense. In conducting research using animals, the investigators adhere to the laws of the United States and regulations of the Department of Agriculture.

Authors and affiliations: Liyuan Zhang, Ph.D., and Barbara St. Pierre Schneider, Ph.D., RN, FAAN, School of Nursing, University of Nevada, Las Vegas, NV; and Julia Soulakova, Ph.D., Burnett School of Biomedical Sciences, University of Central Florida, Orlando, FL.

REFERENCES

1. Abbany Z. Non-stop madness: how long-haul flights affect your mind. Deutsche Welle. 2018. [Accessed July 2019]. Available from: https://www.dw.com/en/non-stop-madness-how-long-haul-flights-affect-your-mind/a-45826380.
2. Aerospace Medical Association, Aviation Safety Committee, Civil Aviation Subcommittee. Cabin cruising altitudes for regular transport aircraft. Aviat Space Environ Med. 2008; 79(4):433–439.
3. As Project Sunrise discussions continue, new Qantas research reveals what customers really want on ultra long-haul flights. The Blue Swan Daily. 2019. [Accessed Aug. 2019]. Available from: https://blueswandaily.com/as-project-sunrise-discussions-continue-new-qantas-research-reveals-what-customers-really-want-on-ultra-long-haul-flights/.
4. Davidson J. Qantas readies for direct flights from Sydney to London. Financial Review. 2019. [Accessed Aug. 2019]. Available from: https://www.afr.com/technology/qantas-readies-for-direct-flights-from-sydney-to-london-20190430-p51igu.
5. Engel S. What's behind the new boom in ultra-long-haul airline flights. Forbes. 2018. [Accessed July 2019]. Available from: https://www.forbes.com/sites/samuelengel1/2018/10/23/in-bird-versus-singapore-airlines-airbus-bird-flies-longer/.
6. Muhm JM, Rock PB, McMullin DL, Jones SP, Lu IL, et al. Effect of aircraft-cabin altitude on passenger discomfort. N Engl J Med. 2007; 357(1):18–27.
7. Reis C, Mestre C, Canhão H, Gradwell D, Paiva T. Sleep and fatigue differences in the two most common types of commercial flight operations. Aerosp Med Hum Perform. 2016; 87(9):811–815.
8. The rise of the ultra-long-haul flight. The Economist. 2018. [Accessed July 2019]. Available from: https://www.economist.com/graphic-detail/2018/03/27/the-rise-of-the-ultra-long-haul-flight.
9. St. Pierre Schneider B, Moonie S, Fulkerson ND, Nicholas J, Bammler T, Voss JG. Simulated flight, muscle genetics, and inflammatory indicators in mice. Aviat Space Environ Med. 2013; 84(8):840–844.
10. Schneider BS, Vigil SA, Moonie S. Body weight and leukocyte infiltration after an acute exercise-related muscle injury in ovariectomized mice treated with estrogen and progesterone. Gen Comp Endocrinol. 2012; 176(2):144–150.
11. Silverman D, Gendreau M. Medical issues associated with commercial flights. Lancet. 2009; 373(9680):2067–2077.
12. Singapore Airlines launches world's longest flight. Singapore Air. 2018. [Accessed July 2019]. Available from: https://www.singaporeair.com/en_UK/gb/media-centre/press-release/article/?q=en_UK/2018/October-December/ne3418-181012.
13. Staples KJ, Sotoodehnejadnematalahi F, Pearson H, Frankenberger M, Francescut L, et al. Monocyte-derived macrophages matured under prolonged hypoxia transcriptionally up-regulate HIF-1α mRNA. Immunobiology. 2011; 216(7):832–839.
14. Thibeault C, Evans AD. AsMA medical guidelines for air travel: stresses of flight. Aerosp Med Hum Perform. 2015; 86(5):486–487.
15. Wilder-Smith A, Mustafa FB, Peng CM, Earnest A, Koh D, et al. Transient immune impairment after a simulated long-haul flight. Aviat Space Environ Med. 2012; 83(4):418–423.

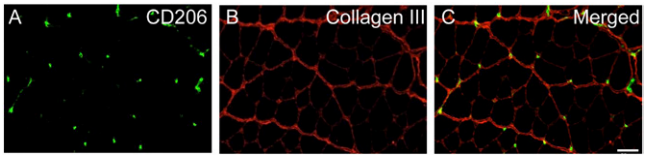

Fig. A1. The separate distribution of A) CD206-positive cells and B) collagen III, and C) the merged distribution of CD206-positive cells and collagen III. Bar = 50 μm.